# Separating the effects of topography and composition in the Clementine UVVIS data set

Paul Withers - 10 May 1999

Remote Sensing of Planetary Surfaces

Topography and surface composition both affect the appearance of a surface image. Deconvolving these two effects will enable a better understanding of the nature of the surface. A technique based on unsupervised classification which uses spectral ratios to identify pixels with similar surface composition is applied to five lunar images. Image resolutions are 100 or 500 m and the sites include the Apollo 16 and 17 landing sites. Shaded relief maps and images corrected for topography are generated for each of the five images. The technique is evaluated by comparing the results to a pre-existing shaded relief map and corrected image for the Apollo 17 site and by examining the effects of the technique on the FeO and $TiO_2$ abundances predicted via the Lucey et al method at the Apollo 16 site. The technique is useful at high phase angle but needs further analysis to become a scientific tool.

# Introduction

"Images of light reflected from a solid surface, in general, contain two kinds of information: (1) spectral-reflectivity variations related to the intrinsic properties (albedo and colour) of materials within the scene, and (2) reflected-intensity variations due to slope or topography that modulate the illuminating flux that is incident on the surface. In the absence of albedo and colour variation, image brightness is a function of topography only." (Eliason et al, 1981)

Figure 1, a lunar crater field, shows the effect of topography in the shading of its craters.

A technique to separate these two kinds of information within an image would be extremely useful, allowing for the calculation of intrinsic albedo and colour and, with some knowledge of the photometric function of the surface, generation of a digital elevation map (DEM). Even without the photometric function a shaded relief map can be generated. Knowledge of intrinsic albedo and colour allows mineralogical studies to be made.

In 1981, Eliason et al proposed such a technique. Assuming that all materials in the scene have the same photometric function and that this photometric function is independent of wavelength for the wavelengths of interest, they wrote

$B(x,y,\lambda) = R(x,y,\lambda) * M_T( T(x,y), \phi(\alpha,i,\varepsilon) )$

where B is the image brightness as a function of position (x,y), R is the brightness of the scene as a function of wavelength, $\lambda$, if the surface were flat, and $M_T$ is the modulation of the brightness introduced by topography; it is a function of the topography, T(x,y), and the photometric function,

$\phi(\alpha,i,\varepsilon)$. $M_T$ is, in effect, a shaded relief map. The photometric function, in turn, depends on the phase angle, $\alpha$, the incidence angle, i, and the emission angle, $\varepsilon$ (Eliason et al, 1981). Atmospheric effects, discussed in their paper, are neglected here. Since $M_T$ is wavelength independent, ratios of B should equal ratios of R. Pixels with similar B ratios are assumed to contain the same surface material and are assigned to the same "cluster". This assumption will not be true if the scene contains different materials with similar colours but different albedos. Slopes of all pixels within such a cluster are assumed to be symmetrically distributed toward and away from the sun, such that their average brightness can be used to estimate the brightness of that material on a flat surface. Once an estimate for R is obtained in this manner, B/R gives $M_T$. Note that as many different $M_T$s can be calculated as there are wavelengths but all should be the same. This provides a quick and simple rejection test. The assignment of pixels to clusters is performed by unsupervised classification, also known as cluster analysis.

The recent Clementine mission to the Moon (Nozette et al, 1994) is in the process of releasing global mosiacs with 500m and 100m per pixel resolution from the UVVIS camera with wavelengths of 415, 750, 900, 950, and 1000 nm. This information is being used by scientists to study the lunar surface mineralogy and the afore-mentioned topographic modulation of the images is impeding progress (e.g. New Moon II session, Lunar Planet. Sci., 30th, 1999). A successful demonstration of this technique on this data set would allow improvements in these studies. This is no current lunar DEM, and generating one from Apollo stereophotography would be a very lengthy process, only giving results in the equatorial region of the Moon. An additional benefit of this technique would be a short cut to creating a global DEM using $M_T$ and a lunar photometric function (McEwen et al, 1998).

This technique has not been widely used following the initial paper. It has been tried and found wanting in a number of situations (McEwen, personal communication, 1999). It is hoped that it will work on the Clementine UVVIS data, which has been carefully calibrated, since the lunar photometric function is independent of surface composition and reasonably independent of wavelength in the range of interest (McEwen et al, 1998).

## Technique

Human input into this technique is more or less limited to choosing the unsupervised classification algorithm. However, there are many, many ways to perform the classificiation. Unsupervised classification is discussed in, e. g., Hartigan, 1975. Most algorithms require the user to specify the final number of clusters obtained. It is important to have enough clusters to capture the diversity of the scene and sufficient pixels within each cluster for the "averaging out of topography" to work. I chose to use ~ 50 clusters and images with ~ 500x500 pixels. IDL contains an unsupervised classification algorithm (clust_wts, cluster) but as it can only handle ~ 33000 (~ 180x180) pixels it was not used.

Internet IDL libraries provided me with one unsupervised classification algorithm which was used with only minor modifications (http://www.astro.washington.edu/deutsch-bin/getpro/library31.html?NN_CLUST and http://www.astro.washington.edu/deutsch-bin/getpro/library31.html?NN_LEARN). This algorithm will be referred to as the "clustering algorithm". The 5 band dataset can provide 4 ratios but as the

900, 950, and 1000 nm bands are very closely correlated I used only 2 ratios - 415/750 and 900/750.

20 iterations were used and both ratios were first normalized to a mean of zero and a standard deviation of unity.

To examine the dependence of the results on the choice of unsupervised classification algorithm I also used a second algorithm for which only the 415/750 ratio was necessary. Pixels with ratio values greater than the first percentile of pixels and less than the ninety-ninth percentile of pixels had their ratio values linearly stretched to a range of 0 to 50. The first percentile of pixels were assigned a ratio value of 0. The ninety-ninth percentile of pixels were assigned a ratio value of 50. The pixels were then assigned into one of 50 clusters depending on whether their stretched ratio value is 0-1, 1-2, etc. This algorithm will be referred to as the "stretch algorithm".

Most of the scenes were passed through a 3x3 low pass filter before classification. This reduced the level of noise in the image. Only the Apollo 16 site, site 2, was examined both filtered and unfiltered.

## Sites examined

The alert reader will have realised that this technique will be best suited to images with significant topographic effects. If applied to an image with insignificant topographic effects it will only degrade the image and generate meaningless shaded relief maps. Hence, I chose to examine sites with large phase angles.

The Apollo 17 site was also studied as Mark Robinson provided me with a DEM (referred to as MSR's DEM) of the site and an 750 nm image corrected for topographic effects using the DEM and a lunar photometric function (figure 2, referred to as MSR's corrected image). The DEM can be converted into a shaded relief map using ISIS' shade command, allowing comparison between this technique and Mark Robinson's results for both the corrected image (figure 2) and the shaded relief map (figure 3, referred to as MSR's shaded relief map). I have not examined whether this command uses a very realistic phase function in detail.

In a series of papers, (Lucey et al, 1995; Blewett et al, 1997; Lucey et al, 1998) Paul Lucey and coworkers have calibrated an algorithm for measuring FeO and $TiO_2$ content remotely from Clementine UVVIS data against returned lunar soil samples. Calculating FeO and $TiO_2$ content at the sample return locations from the pre-processed data and the processed data, and comparing to the actual measurements from returned samples is another means of testing the success of this technique and also a potential application of the technique.

| Site | Scale | Scene size (pixels) | Centre latitude/'N | Centre longitude/'E | Phase angle | Notes |
|---|---|---|---|---|---|---|
| 1 | 500m | 700x350 | 67 | -174 | 58’ | Crater field |
| 2 | 500m | 100x100 | -9.1 | 15.7 | 74’ | Apollo 16 |
| 3 | 500m | 100x60 | 20.1 | 30.6 | 47’ | Apollo 17 |
| 4 | 100m | 500x500 | 21.2 | 29.4 | 22’ | Apollo 17 |
| 5 | 100m | 600x600 | -36.0 | 151.0 | 55’ | Crater field |

Figures 4 - 8 show sites 1 - 5 in the 750 nm band.

These five images were processed as decribed above to generate a corrected image and a shaded relief map.

## Shaded Relief Maps

As discussed above, if the shaded relief maps (SRMs) for a scene do not look the same in each wavelength band then the technique has probably failed. If the shaded relief maps look nothing like shaded relief maps (allowing for possible change in viewing geometry across the scene) then the technique has probably failed. Owing to limitations on disk space, shaded relief maps were not generated for every scene and every wavelength. Here, and later, I use "reasonable" to mean "not obviously incorrect".

| Site | Filtered? | Clustered or Stretched? | Wavelengths for SRMs than x% | SRMs similar? between | SRMs look reasonable? the two | More than 95% of pixels differ by less SRMs |
|---|---|---|---|---|---|---|
| 1 | Yes | Clustered | 415, 750 nm | Yes | Yes | 3% (figure 9) |
| | Yes | Stretched | 415, 750 nm | Yes | Yes | 1% |
| 2 | Yes | Clustered | 415, 750 nm | Yes | Yes | 5% |
| | Yes | Stretched | 415, 750 nm | Yes | Yes | 1% |
| | No | Clustered | 415, 750 nm | Yes | Yes | 5% |
| | No | Stretched | 415, 750 nm | Yes | Yes | 1% |

Bright North Ray and South Ray craters appear bright in SRMs for site 2

| | | | | | | |
|---|---|---|---|---|---|---|
| 3 | Yes | Clustered | 415, 750 nm | Yes | Yes | 5% (figure 10) |
| | Yes | Stretched | 415, 750 nm | Yes | Yes | 1% |

Both shaded relief maps for site 3 compare well to MSR's shaded relief map

| | | | | | | |
|---|---|---|---|---|---|---|
| 4 | Yes | Clustered | 415, 750 nm | Yes | No | 5% (figure 11) |
| | Yes | Stretched | 415, 750 nm | Yes | Maybe | 1% |

Neither shaded relief map for site 4 compares well to MSR's shaded relief map

| | | | | | | |
|---|---|---|---|---|---|---|
| 5 | Yes | Clustered | 415, 750 nm | Yes | Yes | 5% |
| | Yes | Stretched | 415, 750 nm | Yes | Yes | 1% |

Figures 9 - 11 allow comparison of two reasonable (figures 9 - 10) and one unreasonable (figure 11) SRM to the unprocessed images (figures 1 and 9, 6 and 10, 7 and 11).

Shaded relief maps were generated for each wavelength for the filtered site 2 results. All looked reasonable.

| | Clustered | Stretched |
|---|---|---|
| Wavelength/nm | Less than 95% of pixels differ by x% between shaded relief maps for this wavelength and 750 nm | Less than 95% of pixels differ by x% between shaded relief maps for this wavelength and 750 nm |
| 415 | 5% | 1% |
| 750 | n/a | n/a |
| 900 | 3% | 3% |
| 950 | 10% | 10% |
| 1000 | 12% | 12% |

It is difficult to tell if the SRMs are realistic rather than just reasonable without SRMs which are known to be accurate to compare them to. The only comparison I have is to MSR's shaded relief map. This shaded relief map only covers ~10% of sites 3 and 4.

Unsurprisingly, the SRMs for the 415 and 750 nm bands agree best when the classification is performed using just these two bands (stretch algorithm) but the similarity is acceptable in all the examples tabulated. When the SRMs for other bands are considered the agreement is less good. The similarity is unacceptable for the 950 and 1000 nm bands for both algorithms in the two examples given. As expected, the similarity between the 750 and 900 nm is good when the 900 nm band is involved in the classification (clustering algorithm). More surprisingly, it is equally good when the 900 nm band is not involved (stretch algorithm) in these examples.

Disimilarities between SRMs tend to occur inside craters and on crater walls, suggesting that the technique is not handling these areas well. This is unfortunate as many applications of this technique would concentrate on these areas.

## Corrected Images

If the corrected image looks unreasonable then the technique is probably not working as hoped. If the corrected image looks reasonable (e. g. sunlit/shadowed sections of craters corrected), we have no way of knowing if it is working as hoped or not. Exceptions to this are sites 3 and 4 where MSR's corrected image provides a comparison for ~ 10% of the image. The next section on iron

and titanium abundances demonstrates a method of validating which can only be used on scenes containing sample return locations. Only the 750 nm corrected images were examined.

All corrected images look reasonable at first glance. Neither site 3 (figure 12) nor 4 (figure 13) compares well with MSR's corrected image (figure 2), with the most obvious flaw a field of small craters in the valley floor being brightened too much. In the site 5 image (figure 14) many small craters are made more visible. It is not clear whether this is a flaw similar to sites 3 and 4 or a valid correction.

There are differences between images generated by the two classification algorithm, but one is not systematically more reasonable than the other.

## Iron and Titanium abundances

Use of the Lucey et al technique (Lucey et al, 1995; Blewett et al, 1997; Lucey et al, 1998) for remote determination of iron and titanium abundances enables a quantitative test of the validity of the corrected image to be made for scenes containing sample return locations. We have previously seen that neither of the Apollo 17 images are well corrected. In a more detailed project it would be important to quantify the poor correction by comparing pre-processed and post-processed remote determinations of iron and titanium but in this short project I shall omit this step. Consequently I shall only investigate the iron and titanium abundances in the Apollo 16 image, site 2.

First the various sample return locations must be located. Using the report of the Apollo Lunar Geology Investigation Team (1972) I measured the distances to the sample return locations from

the two lower vertices of their station locations map, then converted the coordinates to latitude and longitude using simple geometry and the known latitude and longitude of the lunar module (LM) (8.986'S, 15.496'E; http://nssdc.gsfc.nasa.gov/cgi-bin/database/www-nmc?72-031C). Qview in ISIS was used to identify the pixels corresponding to these locations. It is unlikely that this technique can identify a pixel corresponding to a sample return location with 100% confidence, and a 3x3 pixel box centred on the calculated pixel is probably more realistic. However this will cause many boxes to overlap and give only three non-overlapping sets of boxes. In the interests of maintaining reasonable statistics I decided not to use a 3x3 box and run the risk of having one or two sample return locations misplaced by a pixel. A more accurate means of finding the sample return locations would remove the fear of having a number of locations misplaced. Blewett et al, using 125m per pixel data, used a 3x3 box on most sites, with a larger box when stations were close together.

I used sample return stations 1, 2, 4, 5, 8, 9, and the LM in this work. Stations 3, 7, and 12 are not located on the map; presumably they were planned stops that were omitted from the actual traverse. Station 10 is the ALSEP station which is in the same pixel as the LM. FeO and $TiO_2$ data for station 6 is not given in Blewett et al, making it impossible to compare remote determinations with ground truth. Stations 11 and 13 were omitted in error.

Knowing the pixel containing each of the seven sample return locations listed above, reflectances in the 415, 750, and 950 nm bands can be normalised to the "Adams spectrum" and a 5x5 pixel box centred on the Apollo 16 telescopic standard site (see Blewett et al, 1997 for further details), then used to calculate FeO and $TiO_2$ abundances using the algorithms given in Lucey et al (1998). Since

the $TiO_2$ algorithm in Lucey et al is erroneous (compare their figure 18 to their equation 4) an earlier version of the $TiO_2$ algorithm was used (Blewett et al, 1997)

Calculated FeO and $TiO_2$ abundances from filtered and unfiltered versions of pre-processed, clustered, and stretched data can now be compared to the actual values given in Blewett et al (1997) for the returned soil samples to see if the processing has improved the performance of the algorithm. This is a slightly unfair test. The algorithms are generated using the pre-processed data (admittedly at a different resolution) from these and other sample return locations. A fairer test would be to generate algorithms for each version of the 7 data points and compare fits then. In the interests of a simple, transparent test I decided to use the Lucey/Blewett et al algorithm test, hoping that the fact that the algorithm was generated at a different resolution and with only 20% of its points coming from the Apollo 16 mission would keep it reasonably fair. To further confuse the issue, the Apollo 16 soil samples contain metallic iron contributing to the total iron abundance that the Lucey et al technique is not sensitive to (Blewett et al, 1997). This problem will affect all versions of the 7 data points equally.

Results of the comparisons are quoted as root mean square deviations from the actual values. Comparisons between the two elements may be aided by knowing that FeO abundance is ~ 5wt% and $TiO_2$ abundance is ~ 0.6wt%. The relative error is usually less for FeO than for $TiO_2$.

| FeO error/wt% | Pre-processed | Clustered | Stretched |
|---|---|---|---|
| Filtered | 0.66 | 0.76 | 0.68 |
| Unfiltered | 0.76 | 0.66 | 0.74 |

| $TiO_2$ error/wt% | Pre-processed | Clustered | Stretched |
|---|---|---|---|
| Filtered | 0.37 | 0.09 | 0.15 |
| Unfiltered | 0.49 | 0.34 | 0.27 |

From the FeO results we can see that the processing has not destroyed the fit to the algorithm and seems to have improved it for the unfiltered data. The $TiO_2$ results show startling improvement. Unfortunately, as the $TiO_2$ algorithm used here is only a preliminary version it is not possible to claim great success. A more refined version may not give the same results.

## Conclusions

The results for sites 1 and 5 appear reasonable. It is not possible to say whether they are correct or not without a quantitative test. The results for sites 3 and 4 are not correct. The corrected images are significantly different from MSR's. The results for site 2 appear reasonable, though two craters are too bright in the shaded relief map. The FeO and $TiO_2$ results suggest that they are correct. It would be helpful to compare the FeO and $TiO_2$ results for this "reasonable" site to the same results for the "unreasonable" Apollo 17 site to see if an "unreasonable" result still gives good FeO and TiO2 results.

The sites with the lowest phase angle (i. e. least topographic effects to remove) do not give good results with this technique. Since these probably don't need correcting (compare figures 2, 6, and 7) this is not a problem, though it would be nice to be able to extract some topographic information. It is potentially useful that this technique seems to work where it is most needed - in regions where

high phase angle means large topographic effects. In the Clementine mission, high phase angles occur at high latitudes, precisely where stereo photography for the creation of DEMs is lacking, so the technique is doubly useful.

The two algorithms seem to generate equally good shaded relief maps. Maps in two different wavelengths are most similar when only those two wavelengths are used in the algorithm (stretching) but I do not feel able to conclude that there is no adverse effect on the similarity in other wavelengths based on just two examples. There are differences between the corrected images generated by the two classification algorithm, but one is not systematically more reasonable than the other. The FeO and $TiO_2$ results do not favour one algorithm over the other.

The filtered data provides an improvement in the $TiO_2$ determination, but not in the FeO determination. The unfiltered data is exactly opposite. Shaded relief maps and corrected images were equally reasonable. It is unclear whether filtering provided any improvement or not.

The scattered light problem has not been investigated (Pieters et al, 1994)

Quantitative tests are needed to properly evaluate this technique. It is necessary to quantify what phase angles it will work at, what surface compositions it will work with, exactly how well it will correct images and generate shaded relief maps, and identify suitable classification and filtering algorithms. These are not tasks suited to a semester project. More DEMs and corrected images are necessary for these tasks. One possible approach might be to generate a few fake lunar images using known soil and rock types, suitable topography, and a photometric function. These images

could then be processed by this technique and evaluated against accurately corrected images and shaded relief maps.

This project has shown that this technique is not completely useless. With further evaluation it may be possible to turn it into a useful tool for scientific research.

# References

Apollo Lunar Geology Investigation Team, Documentation and enviroment of the Apollo 16 samples: A preliminary report, US Geol. Survey Interagency Report: Astrogeology 51, (1972)

Blewett, D. T., Lucey, P. G., Hawke, B. R., and Jolliff, B. L., Clementine images of the lunar sample-return stations: Refinement of FeO and TiO2 mapping techniques*, J. Geophys. Res.,* **102**, 16319-16325, (1997)

Eliason, P. T., Soderblom, L. A., and Chavez, P. S. Jr., Extraction of Topographic and Spectral Albedo Information from Multispectral Images, *Photogrammetric Engineering and Remote Sensing*, **48**(11), 1571-1579, (1981)

Hartigan, J. A., Clustering Algorithms, Wiley, New York, (1975)

Lucey, P. G., Blewett, D. T., and Hawke, B. R., Mapping the FeO and TiO2 content of the lunar surface with multispectral imagery*, J. Geophys. Res.,* **103**, 3679-3699, (1998)

Lucey, P. G., Taylor, G. J., and Malaret, E., Abundance and Distribution of Iron on the Moon, *Science*, **268**, 1150-1153, (1995)

McEwen, A., Eliason, E., Lucey, P., Malaret, E., Pieters, C., Robinson, M., and Sucharski, T., Summary of radiometric calibration and photometric normalization steps for the Clementine UVVIS images, *Lunar Planet. Sci., 29th*, 1466, (1998)

McEwen, A. S., and Robinson, M. S., Mapping of the Moon by Clementine, *Adv. Space Res*., **19**(10), 1523-1533, (1997)

Nozette, S. and 34 co-authors, The Clementine Mission to the Moon: Scientific Overview, *Science*, **266**, 1835-1839, (1994)

Pieters, C. M. Staid, M. I., Fischer, E. M., Tompkins, S., and He, G., A Sharper View of Impact Craters from Clementine Data, , *Science*, **266**, 1844-1848, (1994)

Figure 1 => North

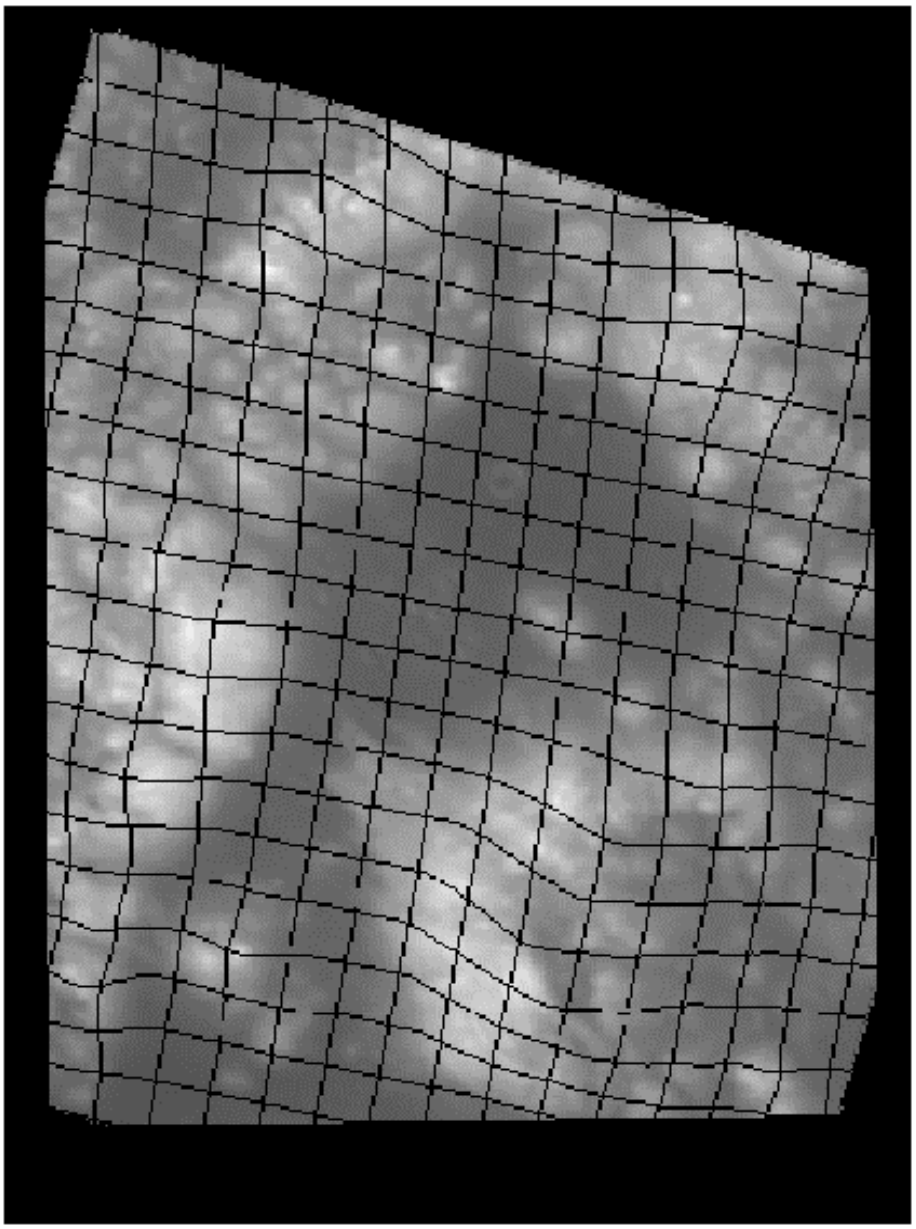

Figure 2 => North

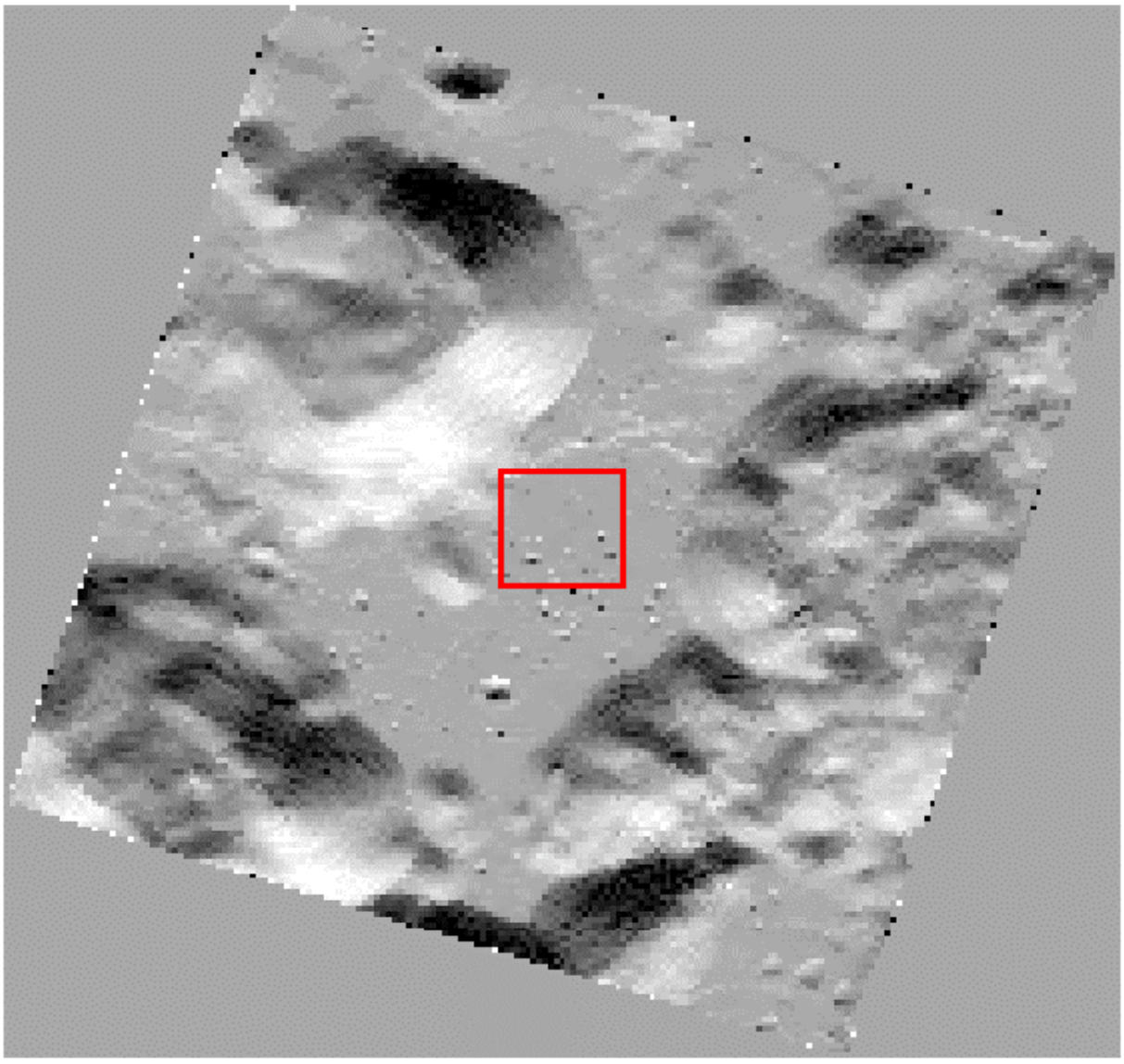

Figure 3 => North

Figure 4 => North

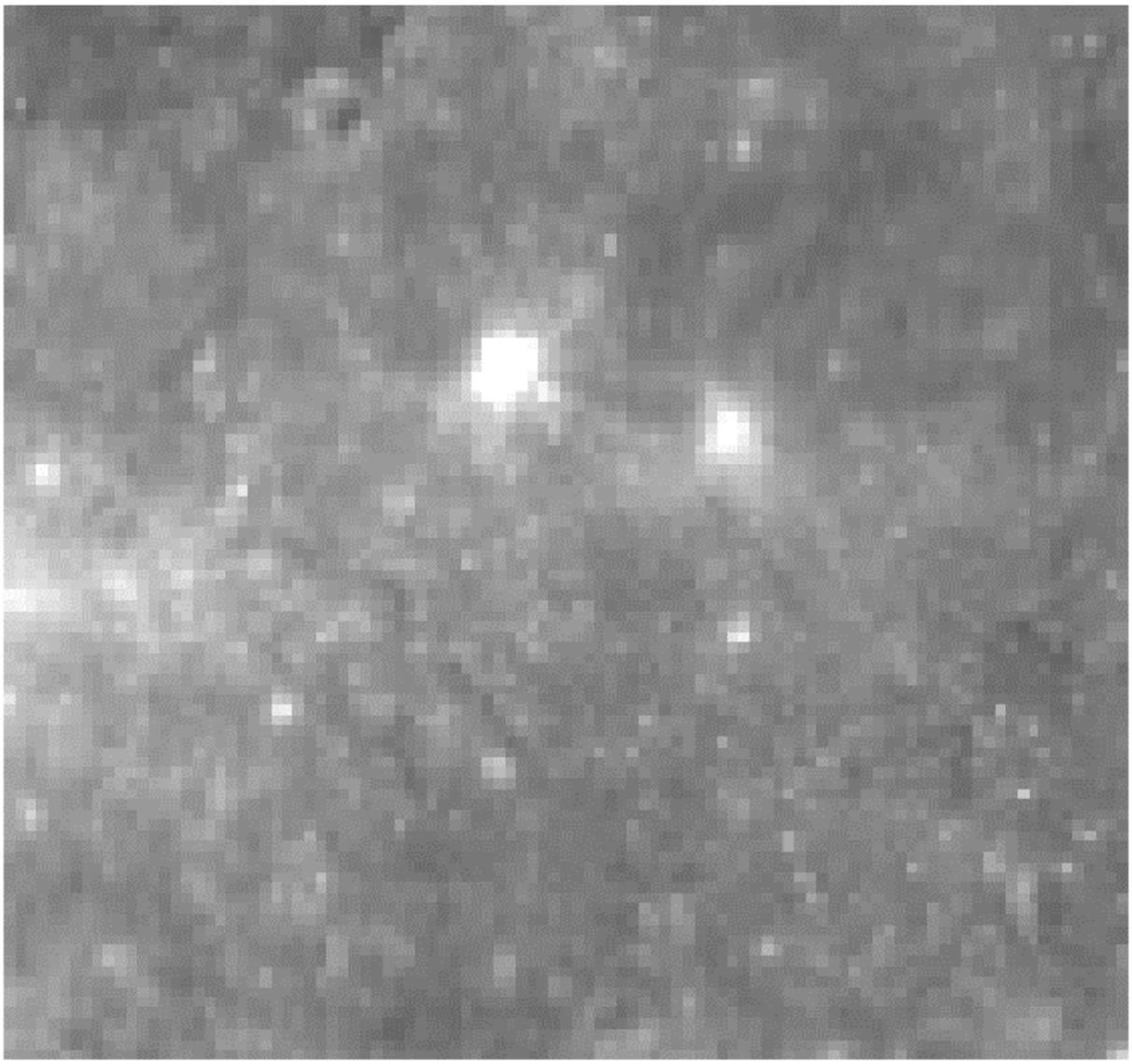

Figure 5 => North

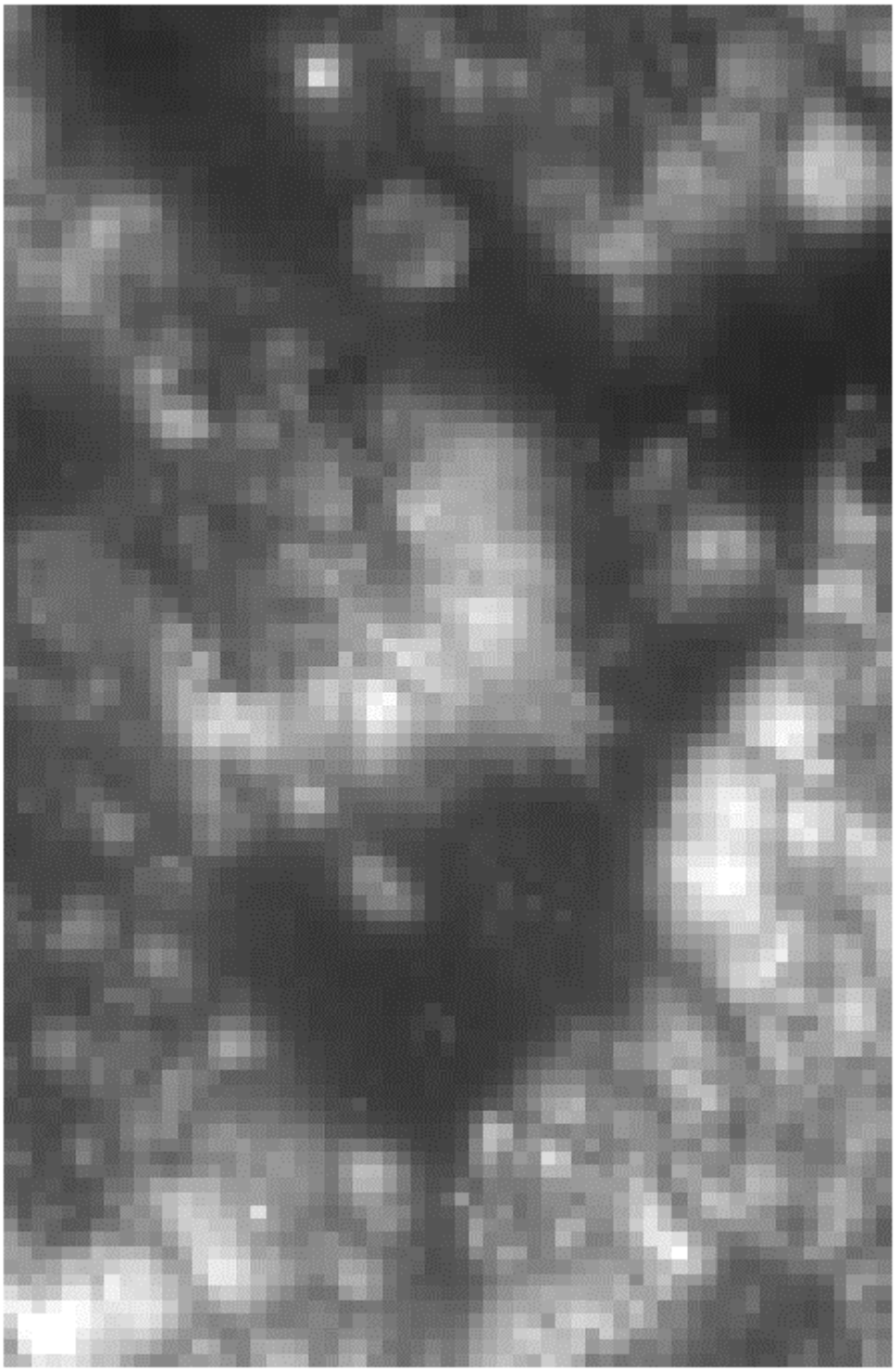

Figure 6 => North

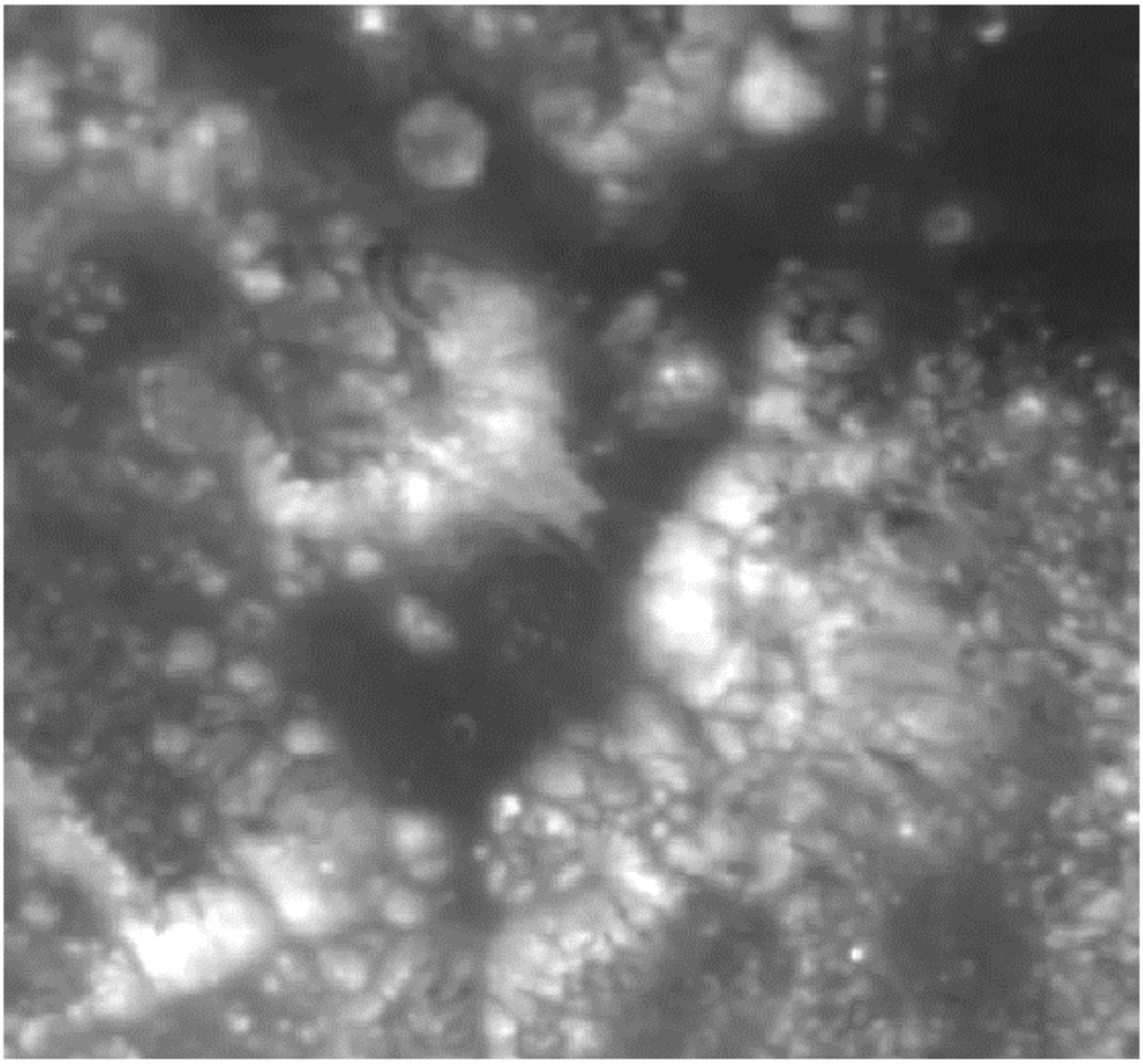

Figure 7 => North

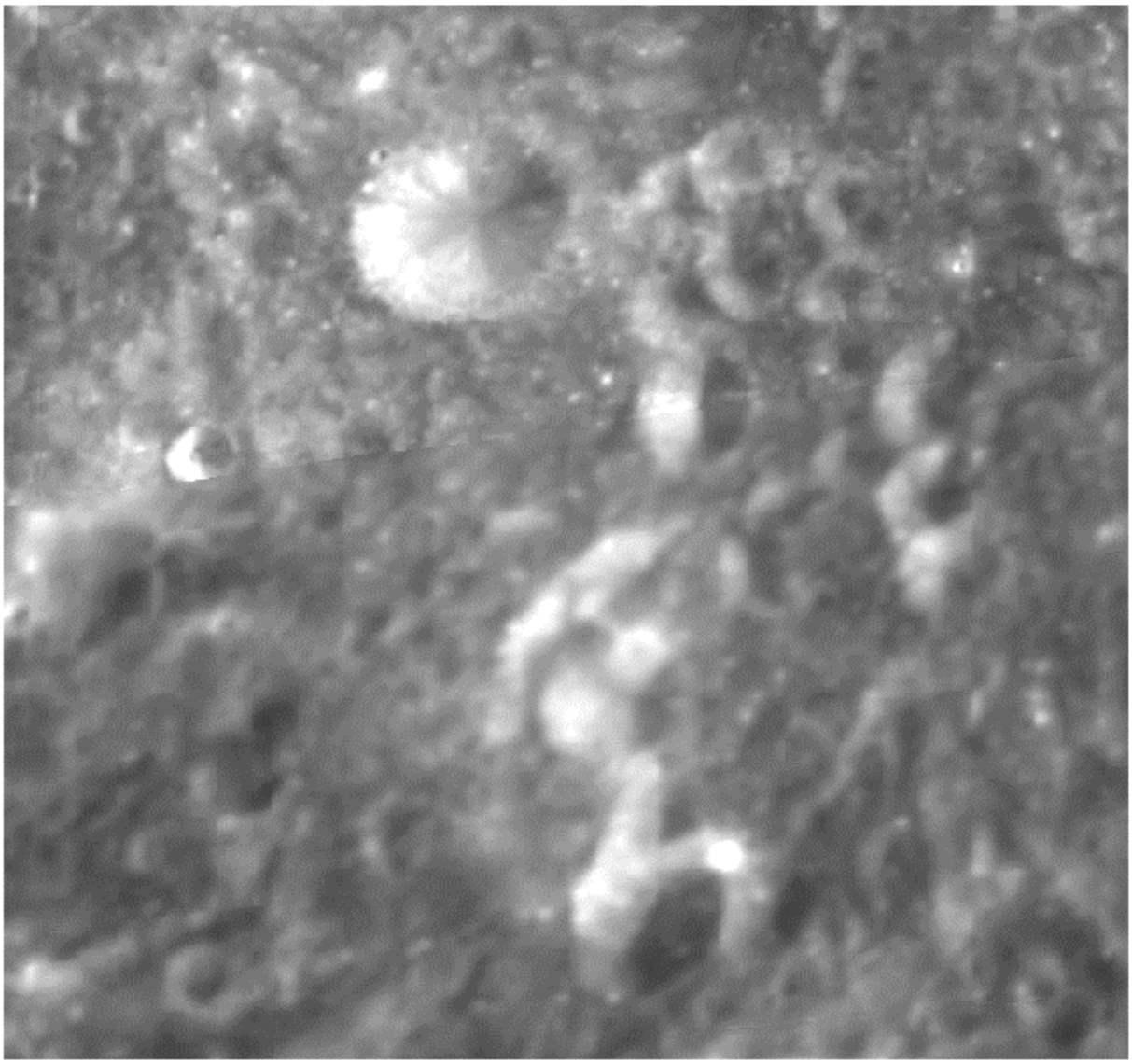

Figure 8 => North

Figure 9 => North

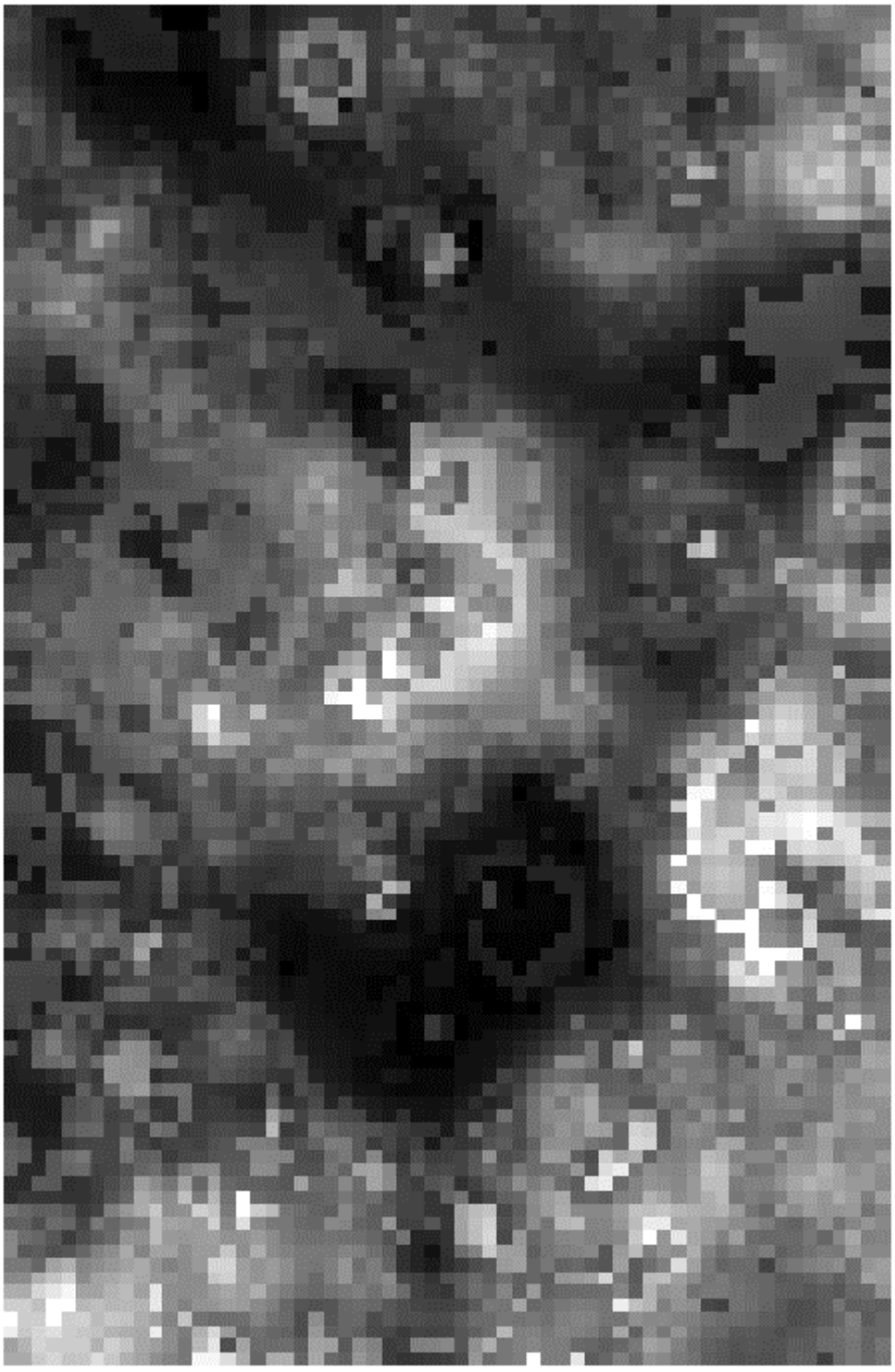

Figure 10 => North

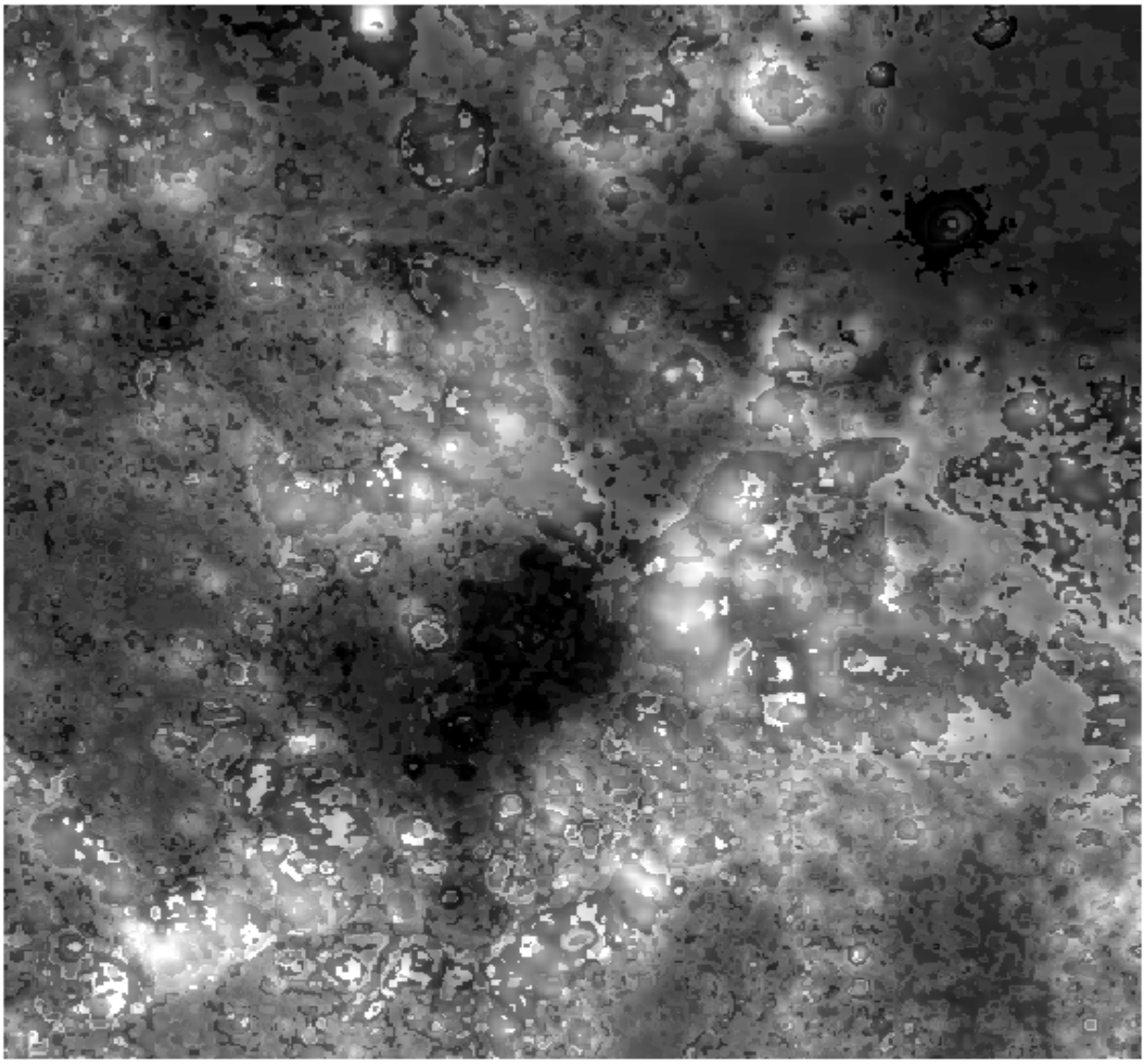

Figure 11 => North

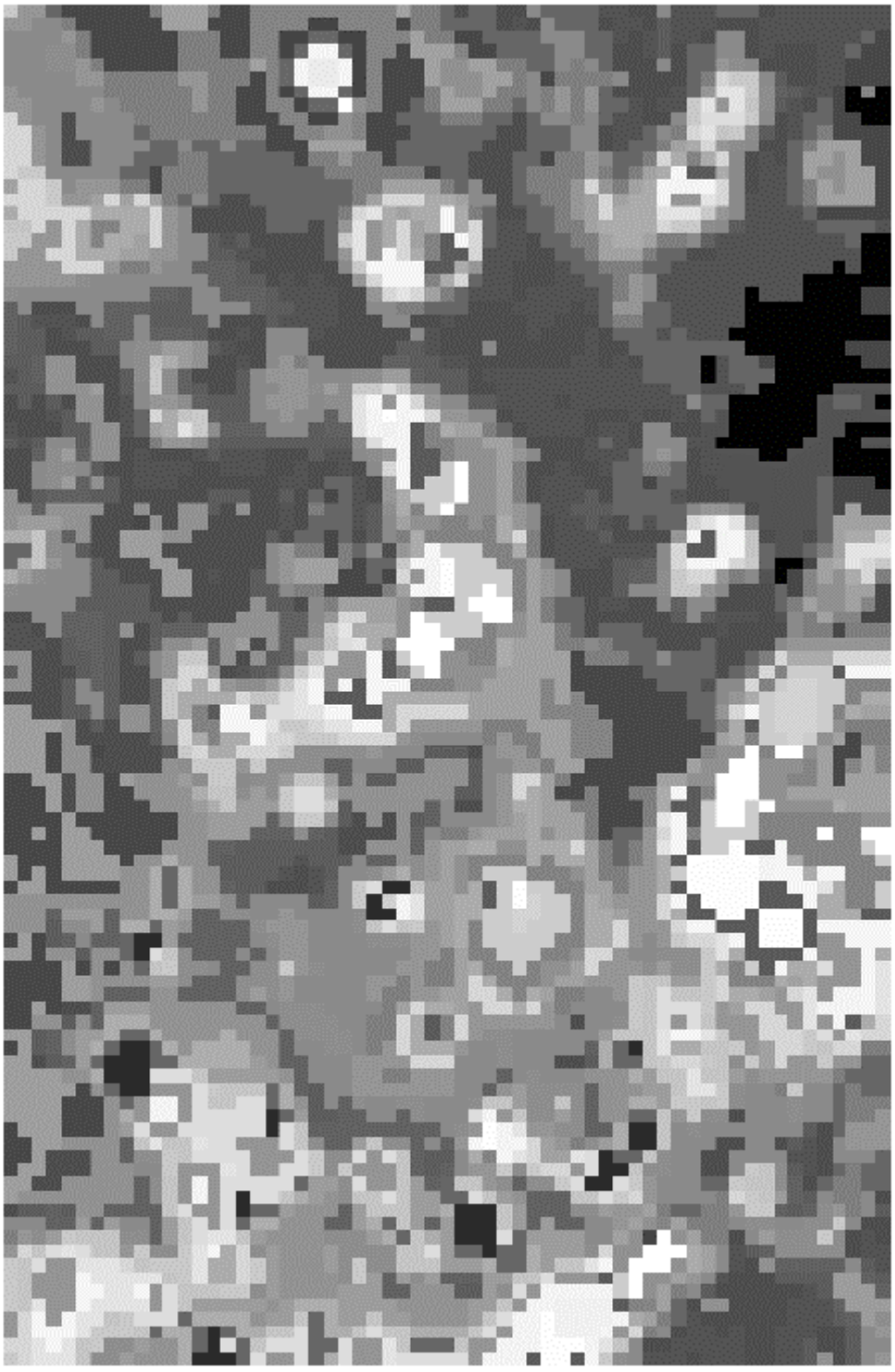

Figure 12 => North

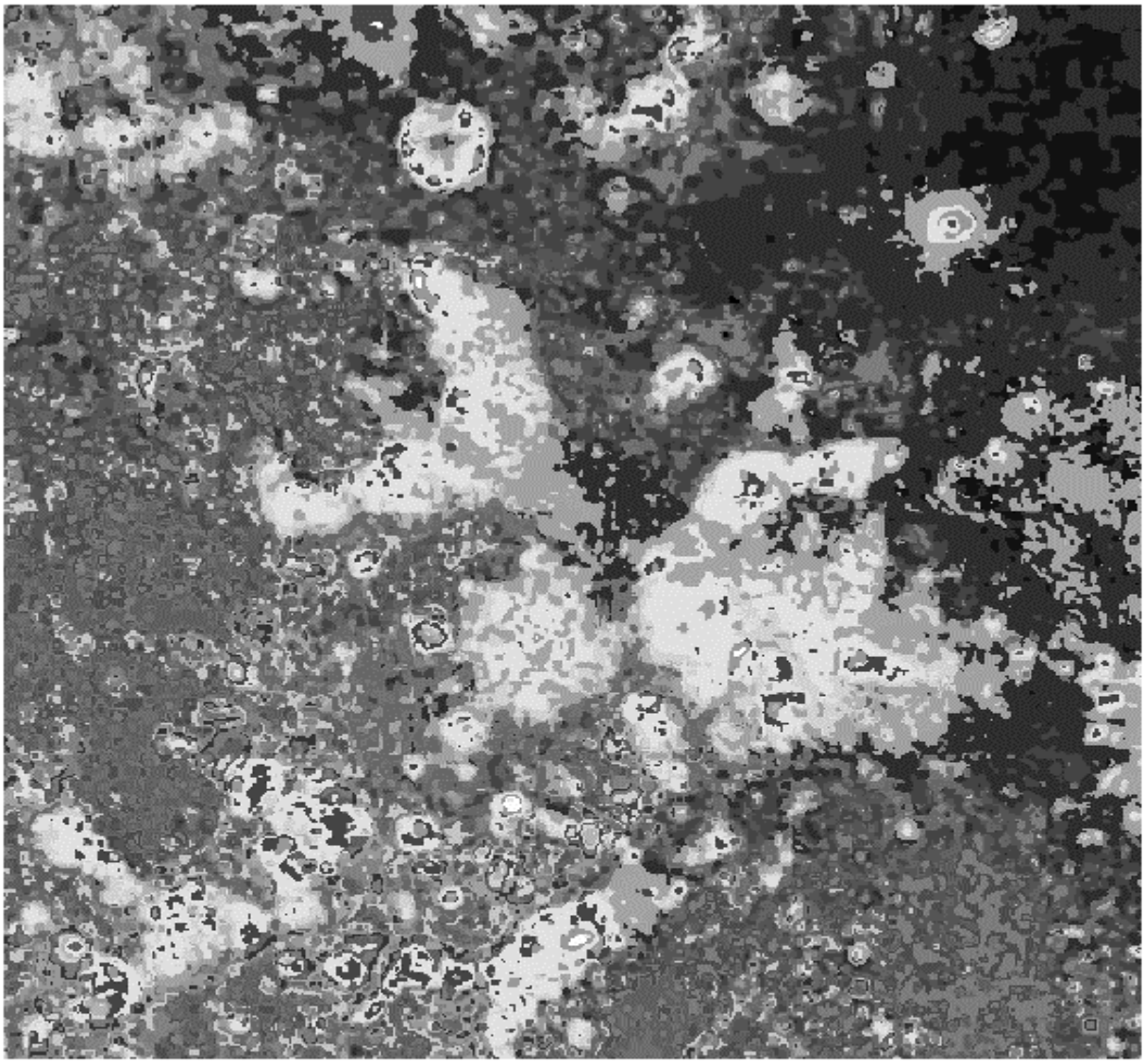

Figure 13 => North

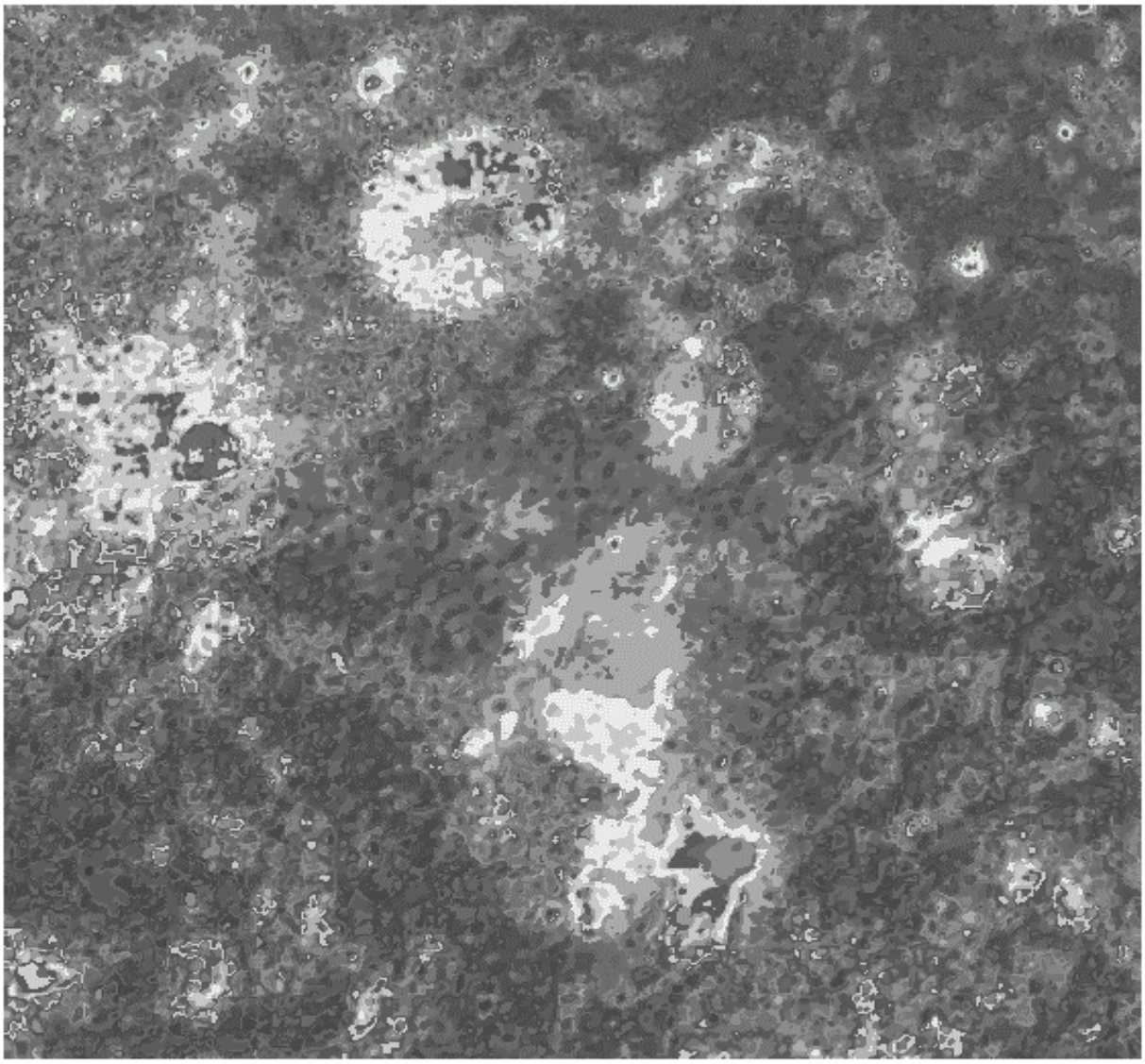

Figure 14 => North